JOURNAL OF AIRCRAFT
Vol. 44, No. 5, September–October 2007

Measured Statistics of Multicomponent Gust Patterns in Atmospheric Turbulence

J. G. Jones*
Stirling Dynamics, Ltd., Clifton, Bristol, BS8 1PG England, United Kingdom

DOI: 10.2514/1.27644

Non-Gaussian statistical properties of severe atmospheric turbulence, recorded at both high and low altitudes, are illustrated by analyzing the outputs of linear filters tuned to respond to multicomponent gust patterns comprising sequences of velocity increments, or "ramp gusts." The measured probability distributions of filter outputs typically have strong tails which can be fitted by a model of exponential form. Although it is known that exponential distributions can be reproduced by considering sequences of Gaussian patches, as assumed in the power–spectral–density method for gust-loads prediction, it is demonstrated, by comparing the outputs of pairs of filters which are tuned to respond to gust patterns comprising different numbers of component increments, that the measured severe turbulence has non-Gaussian properties that cannot be reproduced in this way. In particular, the ratio of the response of a filter tuned to a complex gust pattern to that of a filter tuned to a single-ramp gust varies as a function of gust amplitude, reducing as the amplitude increases. This result is consistent with the hypothesis that the more severe gusts, associated with the tails of the distributions, tend to occur in short "bursts" and is in conflict with the result predicted by the power–spectral–density method, which is that the above ratio is independent of the amplitude. Reference is made to the representation of the burst phenomenon in the statistical-discrete-gust model of extreme turbulence.

Nomenclature

$\bar{A}$	=	measure of system or filter response found by PSD analysis
a_n	=	$N_{0,n}/N_{0,1}$ = zero-crossing ratio predicted by PSD analysis
$a(n;q)$	=	zero-crossing ratio generalizing a_n to non-Gaussian distributions
L	=	incremental distance
$N(X;q)$	=	tangent (in log-linear axes) fitted to $n(X)$ at amplitude q
N_0	=	zero-crossing rate found by PSD analysis
n	=	number of components in complex gust pattern or associated pattern-detection filter
$n(X)$	=	cumulative distribution for peaks of magnitude exceeding X
p_n	=	$\bar{A}_n/\bar{A}_1$ = filter response ratio predicted by PSD analysis
$p(n;q)$	=	filter response ratio generalizing p_n to non-Gaussian distributions
q	=	moment-order parameter (measure of fluctuation amplitude)
$\underline{\Delta u}$	=	velocity difference over distance L
$\overline{\Delta u}$	=	smoothed velocity difference over distance L

I. Introduction

THE statistical method prescribed in the current airworthiness regulations [1] for predicting aircraft loads in atmospheric turbulence, the power–spectral–density (PSD) method [2–4], is based mathematically upon the simplifying assumption that, at least over patches of limited extent, the turbulence can be represented as a stationary Gaussian random process. Furthermore, it is assumed that the patches are of sufficient extent that the associated aircraft response, taken to be linear, may also be treated as a stationary Gaussian random process. For application to structural loads the PSD method introduces the "generalized exceedance expression"

$$\frac{N(X)}{N_0} = P_1 \exp\left(-\frac{X/\bar{A}}{b_1}\right) + P_2 \exp\left(-\frac{X/\bar{A}}{b_2}\right) \tag{1}$$

As detailed by Hoblit [2], subject to the Gaussian-patch assumptions, $N(X)$ is derived theoretically as the rate of crossing, with positive slope, of the given level X by a prescribed load quantity. However, in practice $N(X)$ in Eq. (1) is generally applied [2] as an approximation for the rate of occurrence of *peaks* whose magnitude exceeds the threshold level X. The measure $\bar{A}$ of system response and the zero-crossing rate N_0 are calculated [2] by a linear-response analysis of the given load quantity which combines the system frequency-response function with a prescribed power-spectral density for the turbulence.

Originally, the two terms in Eq. (1) were regarded as applying to nonstorm and storm turbulence, respectively, but this equation has subsequently come to be considered [2] simply as an empirical expression covering all types of turbulence collectively. This is illustrated in sketch t of [2] where graphs illustrating proposed variations of P_1, P_2 (where $P_1 \gg P_2$) and b_1, b_2 (where $b_2 \gg b_1$) with altitude, for use in aircraft loads prediction, are also illustrated. The first term in Eq. (1), representing the nonstorm branch, dominates for small X and the second, representing the storm branch, for large X. Hoblit describes how in practice numerical values of P_1, P_2, b_1, b_2 are derived from flight data by plotting (sketch u of [2]) measured distributions of $N(X)/N_0$ against $X/\bar{A}$, for known values of $\bar{A}$ and N_0, and fitting the first term in Eq. (1) to measured test points at the smaller values of X (nonstorm) and the second term to measured points at the larger values of X (storm).

It follows from Eq. (1) that the *ratios* $p_n = \bar{A}_n/\bar{A}_1$ and $a_n = N_{0,n}/N_{0,1}$ of the quantities $\bar{A}$ and N_0 corresponding to any two linear systems, denoted, respectively, by n and 1, can be used to normalize the associated response distributions to a single universal curve (Appendix). The major result of this paper is that, when applied to measurements of severe turbulence made at both high and low altitudes, it is found to be necessary to replace the above global normalization to a universal curve by a local normalization which is dependent on fluctuation amplitude. To achieve this, it is necessary to replace the ratios $p_n = \bar{A}_n/\bar{A}_1$ and $a_n = N_{0,n}/N_{0,1}$ based on a PSD analysis by associated functions that depend on fluctuation amplitude, reflecting a fundamental non-Gaussian property of the

Received 6 September 2006; revision received 16 February 2007; accepted for publication 17 February 2007.

*Consultant. Senior Member AIAA

turbulence. This result is consistent with the hypothesis that the more severe gusts, associated with the tails of the distributions, tend to occur in short bursts, for which evidence is presented in [5].

Previous indications of the effects of the burst phenomenon on aircraft-response predictions had been presented in [6], which described results of computer simulations of linear aircraft models subjected to inputs comprising measured samples of turbulence. In this study it was demonstrated that the ratio of the magnitudes of the peak responses in the outputs of lightly damped and well-damped systems was less in severe turbulence than in moderate turbulence. However, as the power-spectral densities were of similar shape in the two cases, the PSD method predicted [6] that this ratio would be independent of the severity of the turbulence. The conclusion was drawn that, in the case of inputs in the form of measured severe turbulence, the fluctuations of highest intensity occurred in relatively short bursts whose spatial extent was limited such that the responses of the lightly damped systems did not reach the statistical equilibrium assumed in the PSD analysis. In qualitative terms, any tendency of the turbulence to occur in short bursts will reduce the relative magnitudes of the peak responses of those systems that are tuned to inputs whose spatial extent exceeds that of the burst.

In the case of the statistical–discrete–gust (SDG) model of severe turbulence [5,7], the fact that the most intense fluctuations tend to occur in short bursts is taken into account in terms of empirical complexity factors (or p factors) which, for a prescribed probability of occurrence, define the relative amplitudes of isolated ramp gusts and of more complex gust patterns comprising a number of ramp-gust components. In practice, the p factors are measured by the local normalization, referred to above, which replaces the global normalization based on the ratios $p_n = \bar{A}_n/\bar{A}_1$ and $a_n = N_{0,n}/N_{0,1}$. However, whereas in previous work [5] the measured p factors have been derived by normalizing just the tails of the distributions, the novel method of statistical data analysis employed in this paper, which introduces a nondimensional amplitude metric q which is independent of distribution shape, allows these complexity factors to be quantified as continuous functions of fluctuation amplitude.

To complement the analysis of severe turbulence the same method is applied to an associated Gaussian surrogate process comprising samples (patches) that have power-spectral densities identical to measured samples of severe turbulence but whose phase has been randomized. The significance of the surrogate process lies in the fact that the Fourier representation of a Gaussian process has a random phase distribution, whereas the phase components in the Fourier representation of samples of a non-Gaussian process, such as measured severe turbulence, are correlated. By comparing the responses of linear filters to samples of measured turbulence with the corresponding responses to samples of the related Gaussian surrogate process whose phase distribution has been randomized, but whose power-spectral-densities are *identical* to those of the measured turbulence samples, the significance of phase correlations in the measured turbulence is displayed explicitly.

II. Method of Data Analysis

A. Statistical Distributions of Exponential Type

The basis of the method of data analysis to be described is that the statistics of velocity increments, or two-point differences, in inertial-range turbulence tend to follow probability distributions of exponential type. As early as 1972, Chen [8] illustrated measurements of two-point differences

$$\Delta u(y, L) = u(y + L/2) - u(y - L/2) \tag{2}$$

of turbulence-velocity components $u(y)$ over distances L from four independent data sources, showing that even over patches of limited extent the probability distributions of Δu in the inertial range are typically strongly non-Gaussian, as indicated by strong tails with deviations from Gaussian statistics quantified by large values of the kurtosis. Other measurements of probability distributions of Δu from both experimental and numerical data, showing that within the inertial range these take the form of a stretched exponential, that is, the exponential of (minus constant times) a fractional power of the absolute value of the velocity increment, have been summarized by Frisch [9]. The exponent is typically less than unity, so that the distribution decreases more slowly than exponentially.

Further studies of probability distributions of velocity increments Δu in inertial-range turbulence, with a view to evaluating their significance for the prediction of aircraft response, were presented by Jones et al. [10–12]. In these studies, to achieve a valid comparison between large and small scales (values of L), the measured two-point velocity differences $\Delta u(y, L)$, Eq. (2), were smoothed numerically for subsequent analysis based upon the smoothed-difference function

$$\overline{\Delta u}(y, L) = \int H(x - y, L)\Delta u(x, L)\,\mathrm{d}x \tag{3}$$

where the weighting factor $H(x, L)$ is a smoothing function (low-pass filter) which introduces an average over a distance of order L. As described in [11], $\overline{\Delta u}(y, L)$ may be interpreted as a correlation filter and the occurrence of a specified gust profile in the input detected through the identification of local maxima and minima in the filter output. In particular, it is shown in [11] that the combined smoothing-and-differencing function, Eq. (3), acts as an optimum filter to detect a ramp-shaped gust profile.

Following this approach, scaling properties (dependence upon L) of velocity differences were derived [10–12] from measured local extreme values (maxima and minima) of $\overline{\Delta u}(y, L)$, Eq. (3), with respect to y at chosen values of L. For each such value of L, a cumulative distribution $n(L, X)$ was defined as the average number, per unit distance y, of local extrema in the function $\overline{\Delta u}(y, L)$ having magnitude greater than X and scaling exponents were derived by exhibiting scale-invariant properties of these cumulative distributions.

B. Generalized Filters

In this paper, the above method of data analysis [10–12] is extended to analogous distributions $n(L, X)$ of local extreme values in the outputs of filters which generalize the smoothed-difference function $\overline{\Delta u}(y, L)$, Eq. (3). Just as the function $\overline{\Delta u}(y, L)$ acts [11] as a detector for an isolated velocity increment, it requires only a simple extension of the method to detect more complex gust patterns, represented as linear combinations of ramp-shaped velocity increments, by means of associated linear combinations of smoothing-and-differencing filters. As for single ramps, the occurrence of multiple-ramp patterns is associated with local maxima and minima in the associated filter outputs. However, whereas in previous work [10–12] the primary objective was to investigate the dependence of the distribution $n(L, X)$ upon L, for a filter which detects single velocity increments, Eq. (3), our objective here is to study the dependence of the analogous distributions $n(L, X)$ of extrema in filter outputs upon the complexity of the gust pattern, for prescribed constant values of L, where the complexity of a gust pattern is defined as its number of component increments.

To achieve a rigorous quantitative comparison between the distributions associated with different gust patterns, where the distributions are in general non-Gaussian and may be of different shape, a measure of fluctuation amplitude is required which is nondimensional and independent of the shape of the distribution. In [12] it was shown how such a measure can be defined in the form of a moment-order parameter. Suppose that fluctuations in filter output, of amplitude X, have a probability density function $f(X)$, whose qth moment is given by $\int f(X)X^q\,\mathrm{d}X$. Let X_q denote the amplitude at which $f(X)$ makes its greatest contribution to the qth moment, that is, at which the product $f(X)X^q$ is greatest. Then the resulting stationarity condition

$$X_q = -q\{f(X)/f'(X)\}_{Xq} \tag{4}$$

provides [12] a means of labeling amplitude in terms of q.

In terms of the measured number $n(L, X)$, per unit distance y, of local extrema in the absolute value of filter output having magnitude greater than X, an exponential model of the form

$$n(X) = N_0 \exp(-X/A) \tag{5}$$

is fitted *locally*, over limited ranges of amplitude X, assuming that N_0 and A, in Eq. (5), vary sufficiently slowly with X that they may be regarded as constants within each local range. An advantage of the above exponential model is that moments of all orders exist.

Using Eq. (4), it is shown in [12] that the exceedance rate $n(X)$, modeled by Eq. (5), can be expressed parametrically in terms of the associated moment order q by the pair of equations

$$n(X) = N_0 \exp(-q) \tag{6}$$

$$X = Aq \tag{7}$$

For the purpose of fitting the model to measured data, and comparing distributions from the outputs of different filters, the significance of the above implicit form for the relationship between $n(X)$ and X is that the amplitude variable q is independent of N_0 and A. This is illustrated in a straight-line plot, Fig. 1, of $\log n(X)$ against X, in which changes in N_0, for fixed A, cause a vertical translation of the line, whereas changes in A, for fixed N_0, cause a rotation about a fixed pivot at $X = 0$ equivalent to a stretch of the horizontal axis. Both of these transformations leave the value of q (illustrated) unaltered.

In the following, the exponential model, Eq. (5), is fitted to measured distributions $n(X)$ over local ranges of amplitude, using a minimum-least-squares fit of a straight line to a plot of $\log n(X)$ against X over each prescribed range. This defines a set of tangents $N(X; q)$, Fig. 2, each of which is associated with a particular value of the moment-order parameter q, as in Fig. 2, corresponding to the point of contact (in practice taken to be at the center of the fit range).

In the case of the output of the single-ramp detector, that is, the smoothed-difference function, Eq. (3), the overall form of the distribution $n(X)$ is typically [12] that of a *stretched exponential* [9], which in a plot of $\log n(X)$ against X is concave upwards, as illustrated in Fig. 2. This stretched-exponential distribution $n(X)$ is then completely specified [12] as the envelope of the family of (exponential) tangents $N(X; q)$, parameterized by q and defined by the pair of Eqs. (6) and (7) where now, however, N_0 and A both become functions of q:

$$N(X; q) = N_0(q) \exp(-q) \tag{8}$$

$$X = A(q)q \tag{9}$$

with $N_0(q)$ specifying the intercept with the axis $X = 0$ and $A(q)$ the slope, Fig. 2.

The final step in the method of data analysis is to apply the above procedure to *pairs* of distributions $n(X)$ derived from the outputs of associated pairs of filters, one acting as a detector [based on Eq. (3)] for a single ramp, Fig. 3a, and the other designed to detect a compound gust pattern comprising a sequence of n velocity increments of alternating sign. An example of the case $n = 2$, in which the spacing between the ramps has been chosen to be equal to the ramp gradient distance, is shown in Fig. 3b.

Following Eqs. (8) and (9), we suppose the former distribution, which is interpreted as the datum case, to be specified by a family of tangents:

$$N(X; q) = N_{0,1}(q) \exp(-q) \tag{10}$$

$$X = A_1(q)q \tag{11}$$

and the latter by a family of tangents:

$$N(X; q) = N_{0,n}(q) \exp(-q) = a(n; q)N_{0,1}(q) \exp(-q) \tag{12}$$

$$X = A_n(q)q = p(n; q)A_1(q)q \tag{13}$$

where

$$a(1; q) = p(1; q) = 1 \tag{14}$$

Thus $a(n; q)$ and $p(n; q)$ completely specify the distribution associated with the n-ramp pattern in terms of the single-ramp datum distribution.

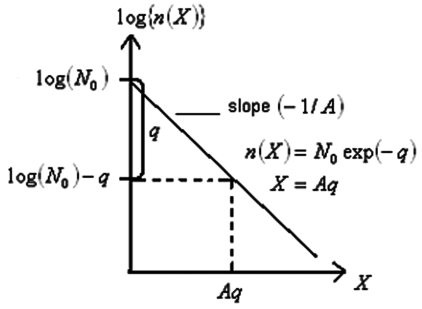

Fig. 1 Illustration of the role of the moment-order parameter q as a dimensionless measure of fluctuation amplitude.

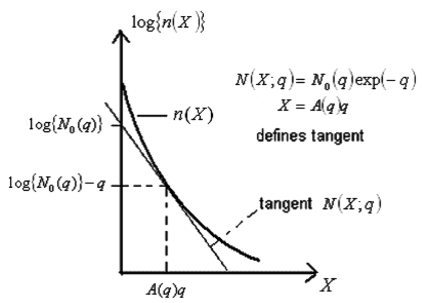

Fig. 2 Tangent to $\log n(X)$ defined by a specified value of the moment-order parameter q.

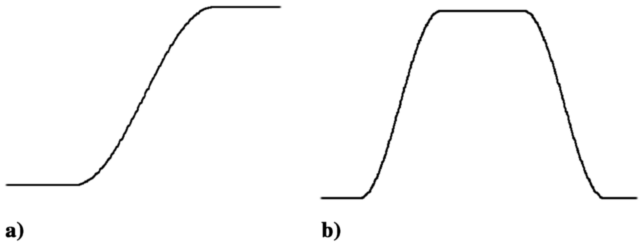

Fig. 3 Typical gust patterns analyzed in present study: a) single isolated velocity increment, or ramp gust; b) compound pattern comprising a sequence of velocity increments of alternating sign.

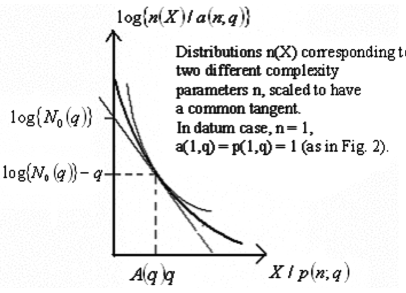

Fig. 4 Pair of distributions $n(X)$ scaled such that logarithmic representations share a common tangent $N(X; q)$, Fig. 2, at a specified value of the moment-order parameter q.

For any such pair of distributions $n(X)$, it follows from Eqs. (10–13) that normalized plots of $\log\{n(X)/a(n;q)\}$ against $X/p(n;q)$, for any chosen value of q, Fig. 4, have a common tangent whose intercept is specified by $N_{0,1}(q)$ and the slope by $A_1(q)$. Following the least-squares procedure described earlier, tangents to the two distributions $n(X)$ are fitted over limited ranges associated with the same value of q and their slopes and intercepts identified. The above normalization to a common tangent then provides an associated set of values of the n-dependent ratios $a(n;q)$, $p(n;q)$.

Applications of the above method of statistical data analysis to derive numerical values of $a(n;q)$ and $p(n;q)$ for a range of n-component sequences of increments are illustrated in the following section for measured severe-turbulence data and also for surrogate data having identical power spectra but random phase. In one class of gust patterns studied, the ramp gradient distances and the spacing between the component ramps, of alternating sign, are chosen to be equal to one another. Such a configuration is illustrated in Fig. 3b for the case $n = 2$. Analogous configurations of sequences of increments corresponding to $n = 4$ and $n = 8$ are also studied. A second class of gust patterns considered comprises sequences of increments, again of alternating sign and having equal gradient distances, with $n = 2$, 4, and 8, but in which the spacing between successive ramps is varied. In the limit as the spacing approaches zero, the resulting patterns take the form of finite segments of a sinusoidal wave having increasing numbers of cycles.

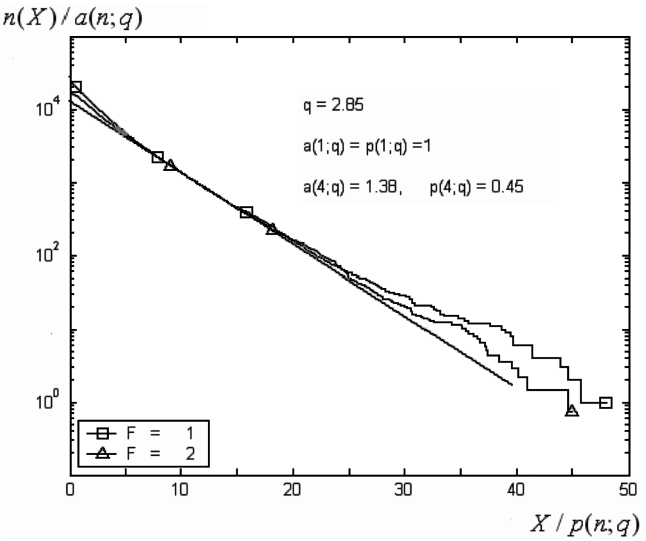

Fig. 5 Application of analysis method illustrated in Fig. 4 to measurements of vertical component of high-altitude turbulence velocity. Filters $F = 1$ and $F = 2$ are detectors for, respectively, a single-ramp gust and a four-ramp gust pattern with ramp lengths and separation between ramps all equal to 20 m.

III. Illustrative Examples

A. High-Altitude Severe Turbulence

The examples of high-altitude severe turbulence are measurements of clear-air turbulence made in 1974/75 at altitudes of approximately 13,000 m (43,000 ft) in the vicinity of the Sierra Nevada ranges in the Western United States in a NASA program [13,14] whose aim was [14] to provide "accurate power-spectral measurements of atmospheric turbulence to wavelengths of the order of 20,000 m (∼65, 000 ft) in an attempt to describe better the power content of atmospheric turbulence." The applicability of the data to the specification of appropriate power-spectral models to be used in aircraft structural load predictions is discussed in [14], which also outlines details of data acquisition and preprocessing, including the extraction and digitization of the longitudinal, lateral, and vertical components of turbulence velocity, and their conversion to functions of position in space using the average true airspeed of each particular run.

The data used here for analysis purposes are taken from a particular flight (flight 32 of [14]) and comprise four data runs (runs 2, 3, 4, and 7) all at an approximate altitude of 13,000 m (43,000 ft) and all containing very severe short-wavelength gusts. For the purpose of the statistical analysis, measurements from the above four data runs have been merged to form a single data block. Because the average true airspeed varies from run to run, the sampling interval of the measured data, which corresponds to a fixed time increment [14], does not transform to a fixed distance in space. Consequently, to achieve a common spatial sampling interval for all four runs within the data block, the measured turbulence components have been resampled to a fixed interval in space, taken to be 2 m. The analysis has been applied to both the vertical and lateral components of turbulence velocity, although the results presented here are for the vertical component only. However, the corresponding results for the lateral component are qualitatively very similar.

A typical example of the output of the analysis program used to derive numerical values for $a(n;q)$ and $p(n;q)$, Eqs. (12) and (13), illustrating the scaling of measured distributions $n(X)$ as in Fig. 4, is shown in Fig. 5 for the case $n = 4$ and $q \sim 3$. The symbols (square and triangle) used in Fig. 5 to identify the two filters also show the ranges of amplitude over which straight-line approximations have been fitted to the two respective measured distributions (in log–linear axes), using a least-squares criterion, as a basis for scaling to derive the common tangent. Figure 5 confirms that, as in Fig. 4, when distributions from two different filters are scaled to have a common tangent at some chosen value of q, for other values of q the scaled distributions in general diverge from one another. This divergence is captured quantitatively by the measured dependence of $a(n;q)$ and $p(n;q)$ upon q.

On the basis of such scaled distributions, Fig. 6 shows measured variations of $a(n;q)$ and $p(n;q)$ for gust patterns with respective numbers of components $n = 2$, 4, and 8, over a range of amplitudes up to $q \sim 4$. In all gust patterns the gradient distances of the component ramps and the spatial separation between ramps are equal to 80 m. Analogous results, which are very similar, have also been obtained for patterns having this characteristic distance equal to 40 m. The second set of results presented, Figs. 7a–7c, shows the effects on $p(n;q)$ of varying the separation between the component ramps for gust patterns with respective numbers of components $n = 2$, 4, and 8 at a prescribed large amplitude of $q \sim 3.5$. The relevant results for high-altitude severe turbulence are coded, respectively, by triangles, for patterns with component gradient distances of 40 m and squares for gradient distances of 80 m. In any given pattern the separations between component ramps are equal and in Fig. 7 this separation is expressed as a multiple of the ramp gradient distance. In all cases there is good agreement between the results for 40 and 80 m, confirming approximate scale independence over this limited range of scales.

B. Low-Altitude Severe Turbulence

The method of statistical data analysis described in Sec. II.B has also been applied to measurements of severe turbulence from a specially instrumented aircraft flying over a variety of types of terrain within the United Kingdom, at low altitudes of between approximately 1000 and 250 ft (300 and 75 m). The turbulence measurement program [15,16] covered a wide range of wind conditions and resulted in segments of flight records covering periods from 60 to 90 s. Details of data preprocessing have been fully described in [15,16] and are summarized in [11]. For the purposes of analysis 25 turbulence-velocity time histories have been selected and combined for analysis into a single data block. This set of time histories has been used previously for analysis in a study [17] of time-phased vertical and lateral gusts, in which the choice was made on the basis that the selected time histories are consistent in both severity and qualitative appearance with those of measured flight records available from airline encounters with severe turbulence [18] at intensities that have sometimes caused injury to passengers and cabin crew as well as large structural loads.

Examples of the chosen time histories, which include instances in which relatively isolated severe gusts occur within a background of turbulence of lower intensity, are illustrated in [17]. As in the case of

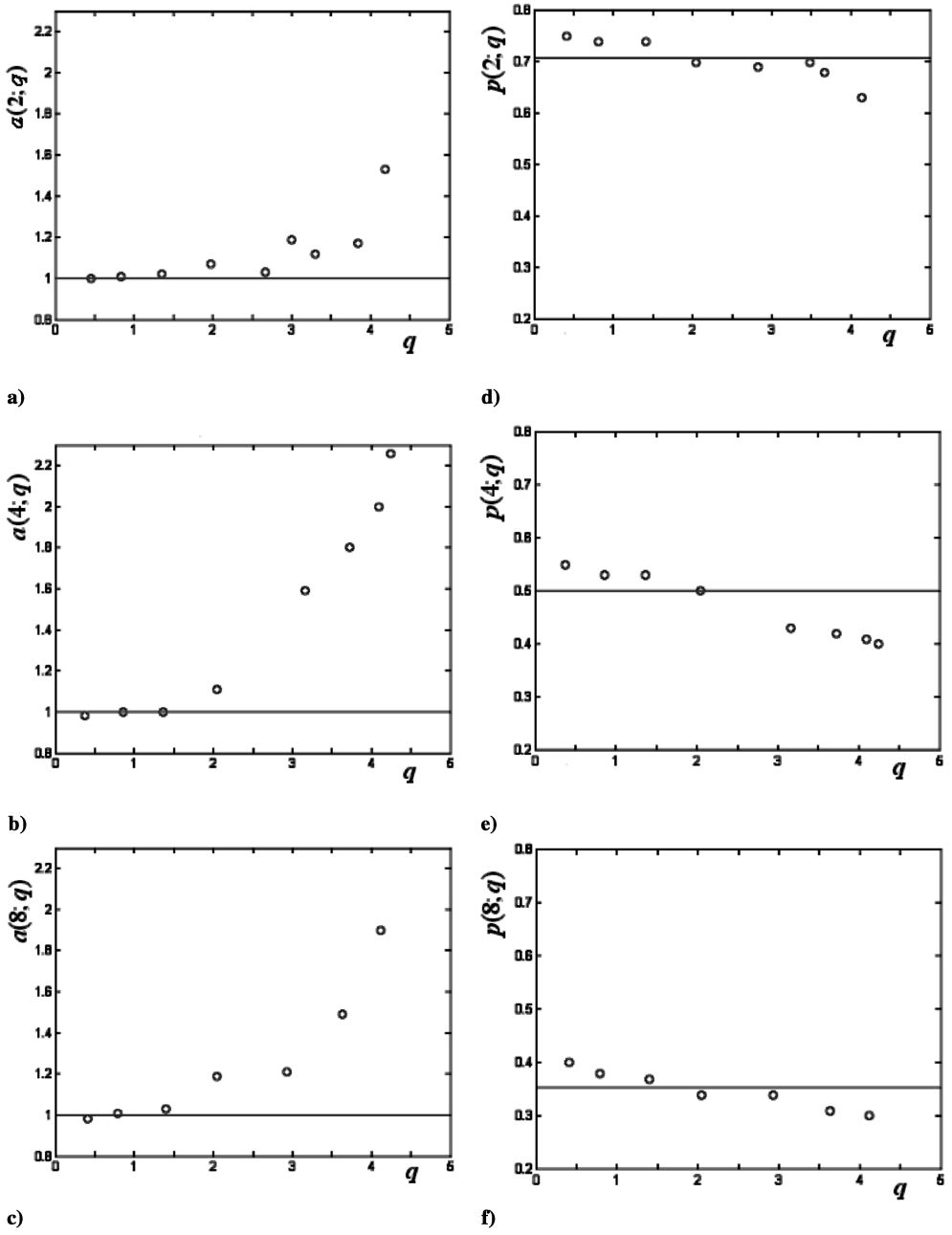

Fig. 6 Measured dependence of $a(n;q)$ and $p(n;q)$ upon moment-order parameter q for gust patterns in high-altitude severe turbulence having numbers of components $n = 2$, 4, and 8. Gradient distances of component ramps and separations between ramps all equal to 80 m. Reference levels for $a(n;q)$ and $p(n;q)$ are unity and $n^{-1/2}$, respectively.

the high-altitude data described in Sec. III.A, each run has been resampled to a common incremental distance of 2 m. Results are presented here for the lateral component of turbulence velocity. Although the corresponding results for the vertical component are very similar, previous work has shown [15,16] that, at the low altitudes at which these measurements were made, due to the influence of ground proximity the lateral component exhibits consistency with the classical $(-5/3)$ form of the power spectral density in the inertial range over a wider range of scales.

Figures 8a–8c show measured variations of $p(n;q)$ with q for gust patterns having respective numbers of components $n = 2$, 4, and 8, over a range up to $q \sim 4$. In these gust patterns the gradient distances of the component ramps and the spatial separation between ramps are all equal to 40 m. At this scale the gust patterns can be shown to lie well within the inertial range [15,16] (it may be noted, however, that the inertial range for these low-altitude data tends to be more restricted than is the case for the high-altitude data). The illustrated dependence of $p(n;q)$ upon q agrees well with that for high-altitude turbulence shown in Figs. 6d–6f.

Further comparisons between the low-altitude and high-altitude results are presented in Figs. 7a–7c, which show the effects on $p(n;q)$ of varying the separation between component ramps in the chosen gust patterns. The results for low-altitude turbulence, which are for patterns with component gradient distances of 40 m, are coded by stars. It can be seen that there is again very good agreement between these results for low altitude and those for high altitude already described in Sec. III.A.

C. Surrogate Data with Randomized Phase

In the following, as a basis for comparison, results are also presented for a set of related surrogate Gaussian signals, obtained by randomizing the phase of the Fourier coefficients of each of the 25 measured turbulence-velocity components analyzed in Sec. III.B.

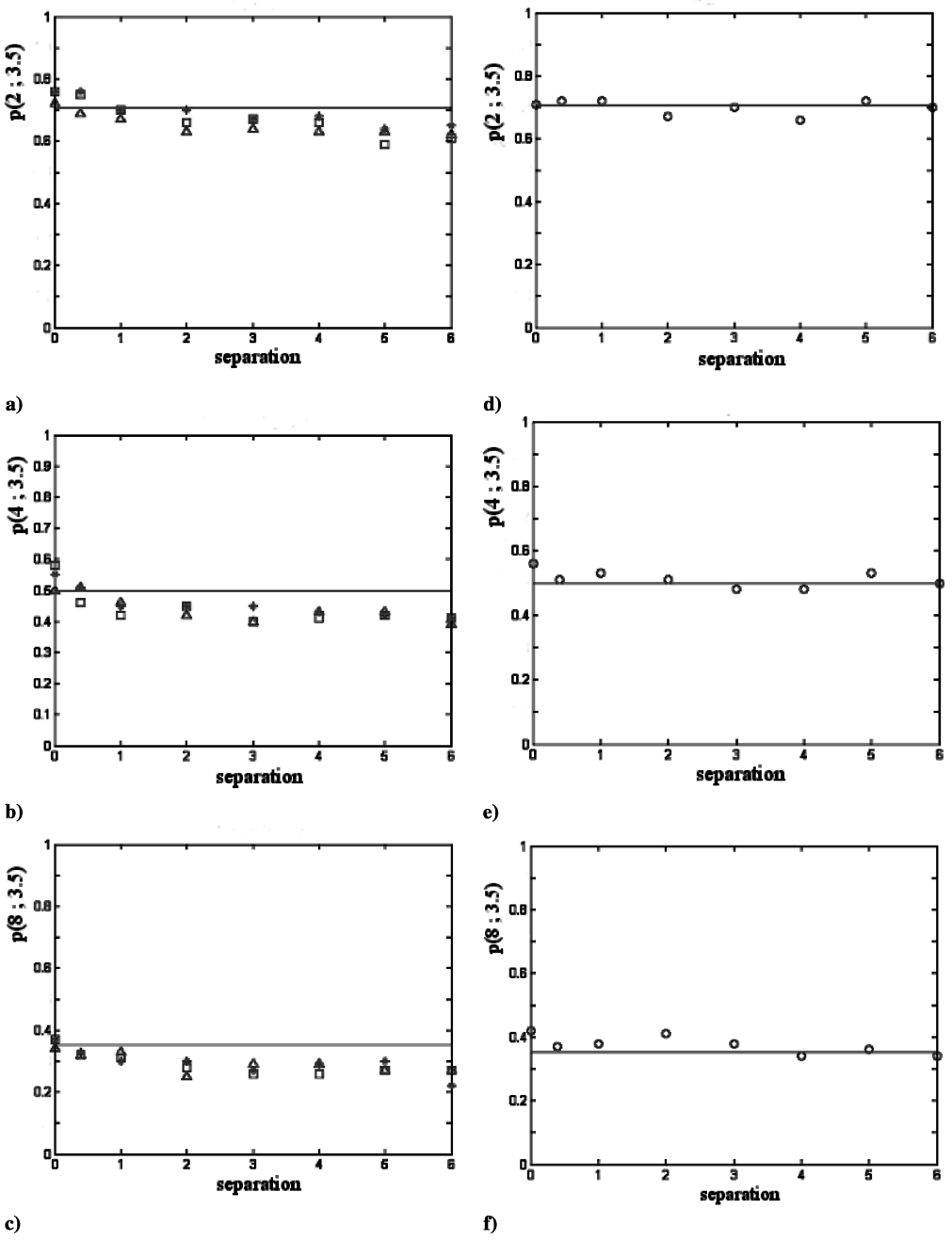

Fig. 7 Measured dependence of $p(n;q)$ upon separation between component ramps, in units of ramp gradient distance, for large-amplitude gust patterns ($q \cong 3.5$) having numbers of components $n = 2$ a) and d); $n = 4$ b) and e); and $n = 8$ c) and f). Symbol code: triangle: high-altitude severe turbulence, gradient distance 40 m; square: high-altitude severe turbulence, gradient distance 80 m; star: low-altitude severe turbulence, gradient distance 40 m; circle : surrogate process with randomized phase, gradient distance 40 m.

The transformation applied involves taking the Fourier transform of each measured turbulence component, retaining the amplitude component of this Fourier transform but replacing the true phase component by a purely random phase component, and finally applying an inverse Fourier transform to generate the required surrogate signal. A MATLAB routine to implement this transformation is given in [19].

The resulting 25 signals are Gaussian, with power-spectral densities identical to those of the measured turbulence components. Thus this ensemble of signals is similar to the Gaussian-patch model assumed in the PSD method of loads prediction [2], but with the idealized von Kármán form of power-spectral density assumed in that model replaced by the true spectral densities of the measured severe turbulence. As shown in the Appendix, the application of the data-analysis method used in this paper to the Gaussian-patch model is amenable to exact theoretical treatment, providing reference values with which the measured properties of the severe turbulence, and of the surrogate data with random phase, may be compared.

Figures 8d–8f show the measured variation of $p(n;q)$ with q for the same set of gust patterns as used in the analysis of severe turbulence, Figs. 8a–8c. Further comparisons between the results obtained for measured severe turbulence and for the associated results from the ensemble of phase-randomized signals are presented in Fig. 7, which shows the effects on $p(n;q)$ of varying the separation between component ramps in the chosen gust patterns. The results for the phase-randomized signals, which are for patterns with component gradient distances of 40 m, are coded by circles.

IV. Discussion

The measured dependence of both $a(n;q)$ and $p(n;q)$ upon amplitude q, in high-altitude severe turbulence, is illustrated in Fig. 6

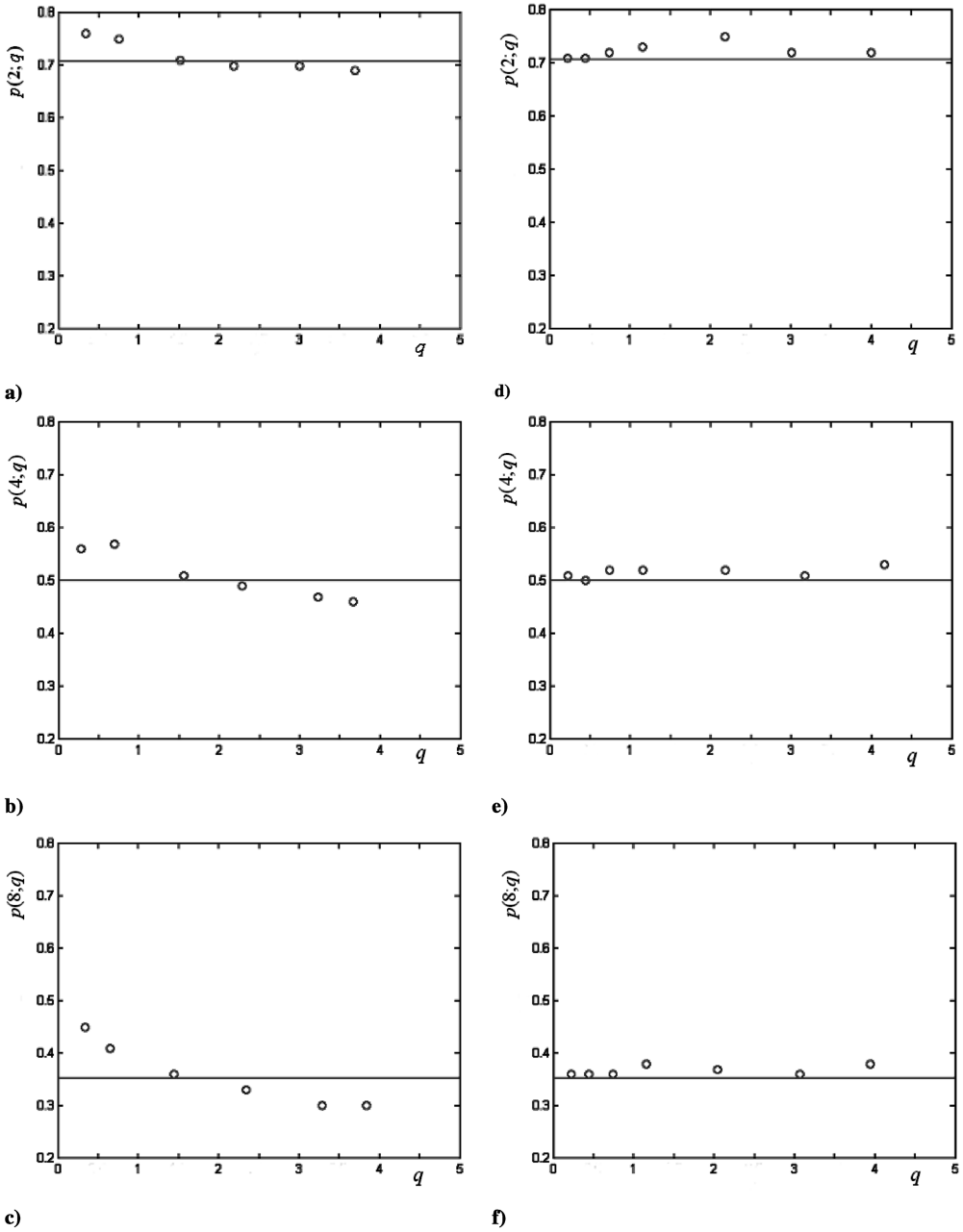

Fig. 8 Measured dependence of $p(n;q)$ upon moment-order parameter q for low-altitude severe turbulence a)–c) and surrogate process with randomized phase d)–f). Gust patterns have numbers of components $n = 2$ a) and d); $n = 4$ b) and e); and $n = 8$ c) and f). Gradient distances of component ramps and separations between ramps all 40 m.

for gust patterns having numbers of components $n = 2, 4$, and 8. As shown in the Appendix, in the Gaussian model these functions become independent of q. The datum amplitudes for $a(n;q)$ and $p(n;q)$ shown as horizontal straight lines in Fig. 6 correspond to the constant theoretical values, of unity and $n^{-1/2}$, respectively, applicable [5] to the particular Gaussian process having PSD proportional to (frequency)$^{-2}$, corresponding to the higher-frequency range of the Dryden spectrum sometimes used as a simplifying approximation in aeronautical applications [2]. The results illustrated in Fig. 6 show that, in severe turbulence, relative to the response of the single-ramp filter, the responses of the more complex filters ($n = 2$, 4, 8) exhibit statistically significant departures from the predictions of the PSD theory. Specifically, the measured strong dependence of both $a(n;q)$ and $p(n;q)$ upon the fluctuation amplitude, as quantified by q, conflicts with the prediction that these quantities take constant values $a_n = N_{0,n}/N_{0,1}$ and $p_n = \bar{A}_n/\bar{A}_1$ [Eqs. (A1) and (A2) of the Appendix]. A comparison of the results in Figs. 6d–6f with those illustrated in Figs. 8a–8c confirms that a similar dependence of $p(n;q)$ upon q is also exhibited in low-altitude severe turbulence.

On the other hand, direct confirmation of the predictions of PSD theory is provided by the results in Figs. 8d–8f, which illustrate measured values of $p(n;q)$ for the surrogate process with randomized phase, which consists of a sequence of Gaussian patches. For each gust pattern, $n = 2$, 4, and 8, a comparison of the respective results [a) with d), and so on] shows that an effect of phase randomization is to remove the trend, observed in the case of the measured severe turbulence, in which $p(n;q)$ decreases as q increases from low ($q \sim 0.5$) to large ($q \sim 3.5$) values. The measured values in Figs. 8d–8f are consistent with the theoretical result (Appendix) that for the Gaussian-patch model $p(n;q)$ is independent of q.

Figure 7 illustrates effects of separation between component ramps of large-amplitude gust patterns, with the values of $p(n;q)$

remaining approximately constant over separation ratios from 2 to 6, at a level significantly below the datum amplitude (horizontal line) corresponding to the theoretical (Gaussian) value of $n^{-1/2}$, but increasing as the separation ratio is reduced from 2 to zero, at which value the patterns become purely sinusoidal. It can be seen, in Fig. 7, that an effect of phase randomization is to remove any significant dependence of $p(n;q)$ upon the separation between the component ramps of the respective gust patterns, this result being consistent with the simple theoretical model (referred to in Sec. III.A) upon which the datum reference values (horizontal lines) are based.

Figures 6–8 demonstrate that, at the higher levels of fluctuation amplitude ($q \geq 3.5$), the ratio of the response of a complex filter ($n \geq 2$) to that of a single-ramp detector, given by $p(n;q)$, is less in severe turbulence than the corresponding ratio $p_n = \bar{A}_n/\bar{A}_1$ associated with the PSD Gaussian-patch model and also that measured for a sequence of patches with randomized phase. This result is taken into account in the SDG model of turbulence [7], proposed as an alternative to the PSD method as a basis for aircraft loads prediction [5]. In the SDG model each aircraft load is related to an associated discrete tuned gust pattern which produces the maximum response from within a wide range of equiprobable gust patterns, each synthesized as a combination of ramp components. The above result concerning the values of $p(n;q)$ then carries over to the ratio of two aircraft loads, one tuned to an isolated ramp gust and the other to a more complex gust pattern.

In the SDG model the response ratios $p(n;q)$ appear as complexity factors (or p factors) [5] which, for a prescribed probability of occurrence, define the relative amplitudes of isolated ramp gusts and of more complex gust patterns comprising a number n of ramp-gust components. In previous descriptions [5] of the SDG model the continuously varying amplitude parameter q has not appeared explicitly. Instead, the model has primarily been proposed [5] as a basis for a design criterion for structural loads in extreme turbulence, in which case the proposed p factors correspond to values of $p(n;q)$ evaluated, using the method of scaling measured statistical distributions as employed in this paper, for large values of q.

Alternatively, using a different set of p factors, chosen to match the response ratios $p_n = \bar{A}_n/\bar{A}_1$ derived from the PSD model (Appendix), it has been demonstrated previously that an equivalence, or overlap [20,21], exists between the predictions of system response obtained using the PSD and SDG models. However, when the p factors associated with severe turbulence are substituted, significant differences arise between the aircraft loads predicted by the PSD and SDG models [5].

Although p factors associated with the tails of distributions obtained from measured severe turbulence have been documented [5] in previous work, the present paper is the first to demonstrate how values of the response ratio $p(n;q)$ can be evaluated as functions of an independent metric, the moment-order parameter q, over a continuous range of fluctuation amplitudes. It has been shown how this provides a bridge between the related amplitude-independent measure $p_n = \bar{A}_n/\bar{A}_1$ associated with the PSD method, which is well matched by values of $p(n;q)$ measured for values of q of order 2 (second-order moments), and the p factors proposed for the SDG model of extreme turbulence which correspond to values of $p(n;q)$ measured for large values of q (of order 4).

This bridge between the PSD and SDG models, provided by the variation of q over a continuous range of fluctuation amplitudes, complements that established in previous work [12] where the moment-order parameter is used to specify an amplitude-dependent scaling exponent $k(q)$ in a multifractal SDG model which matches the PSD model (in which $k = 1/3$) for small values of q and the SDG model of extreme gusts (in which $k = 1/6$) for values of q of order 4. Thus, with appropriate choice of q, the SDG model may be used to represent either continuous turbulence or relatively isolated gusts. The limitations of the PSD model and the relative advantages of the SDG model as a representation of important features of atmospheric turbulence have been noted in [22], in which the SDG model is fitted to tower-based atmospheric turbulence data using both the smoothed-difference function, Eq. (3) of the present paper, and wavelet analysis. Very good matching is noted between the results of the two analysis methods. The use of wavelet analysis as an alternative method for extracting gust structure in atmospheric turbulence data, in a form consistent with the SDG model, has also been described in [11].

V. Conclusions

1) The PSD method for gust loads prediction involves the calculation of two basic quantities: a measure of system response $\bar{A}$ and a zero-crossing rate N_0. It follows from the associated theory, based on the assumption that turbulence can be represented as a sequence of continuous Gaussian patches, that the ratios $p_n = \bar{A}_n/\bar{A}_1$ and $a_n = N_{0,n}/N_{0,1}$ of these quantities for any two linear systems, denoted, respectively, by n and 1, can be used to normalize the associated response distributions to a single universal curve.

2) In contrast, it has been shown, by comparing the responses of linear filters designed as detectors for gust patterns having, respectively, 1 and n ramp components, that when applied to measurements of severe turbulence made at both high and low altitudes it is necessary to replace the above global normalization by a local normalization which is dependent on fluctuation amplitude. Specifically, it is found to be necessary to replace the respective constant normalizing ratios p_n and a_n by response ratios $p(n;q)$ and zero-crossing ratios $a(n;q)$ which depend on the amplitude of response, expressed in terms of the moment-order parameter q, a nondimensional amplitude metric which is independent of the shape of the distributions. In terms of the functions $p(n;q)$ and $a(n;q)$ it has been shown that the respective response distributions can be normalized locally, in the sense of having common tangents (in log–linear axes), at each value of q.

3) When measured at the tails of the distributions (large q), the response ratios $p(n;q)$ are in general reduced relative to the same ratios measured at lower amplitude (small q). This result is consistent with the hypothesis that the more severe gusts, associated with the tails of the distributions, tend to occur in short bursts and is in conflict with the result predicted by the PSD method, which is that the above ratios are independent of the fluctuation amplitude. In consequence, at large gust amplitudes the PSD method tends to overestimate loads associated with the more complex gust patterns.

4) Values of the response ratios $p(n;q)$ measured for large values of q (of order 4) can be identified with the complexity factors, or p factors, used in the SDG model of extreme turbulence [5] to quantify the loads associated with complex gust patterns. For values of q close to 2 (second-order moments) the measured response ratios $p(n;q)$ take values very close to the corresponding response ratios p_n derived from a PSD analysis. For intermediate values of q, $p(n;q)$ provides a continuous bridge between the response predicted by the SDG model of extreme turbulence and the results of a PSD analysis.

5) Consistent results have been derived from the high- and low-altitude severe-turbulence data, supporting previous use [17] of low-altitude data to derive properties of severe turbulence for use in a multi-axis gust model.

6) When applied to a surrogate phase-randomized process, which comprises a sequence of Gaussian patches, the measured response ratios $p(n;q)$ and zero-crossing ratios $a(n;q)$ have been shown to become independent of q, consistent with predictions based on the PSD model.

7) When the spacing between component ramps tends to zero, and the n-component gust patterns considered become segments of a sinusoid, there is a significant increase in the measured response ratios $p(n;q)$. Overall, the results support the conclusion, reached previously in [5], that measured data for severe turbulence are consistent with a discrete gust model which contains a periodic component, in addition to other gust patterns which satisfy the property that their probability is independent of the spacing between their component ramps.

Appendix: Application of Analysis Method to Gaussian-Patch Model

The application of the statistical analysis method of Sec. II.B to the Gaussian-patch model used in the PSD method of loads prediction [2–4] provides a datum with which to compare the measured properties of high- and low-altitude turbulence presented in the main text.

Equation (1) of the main text shows how, in the PSD method, the measure $\bar{A}$ of system response and the zero-crossing rate N_0 influence theoretically the statistical distribution of the response expressed as the sum of two exponentials. Supposing now that $\bar{A}_1$ and $N_{0,1}$ denote values of $\bar{A}$ and N_0 corresponding to some prescribed datum linear system/filter and that $\bar{A}_n$ and $N_{0,n}$ refer to the nth. system/filter in some arbitrary sequence, define

$$p_n = \bar{A}_n/\bar{A}_1, \qquad (p_1 = 1) \tag{A1}$$

and

$$a_n = N_{0,n}/N_{0,1}, \qquad (a_1 = 1) \tag{A2}$$

Substituting from (A1) and (A2) into Eq. (1) of the main text, there is obtained for the nth system:

$$\frac{N(X)}{N_{0,1}a_n} = P_1 \exp\left(-\frac{X}{b_1\bar{A}_1 p_n}\right) + P_2 \exp\left(-\frac{X}{b_2\bar{A}_1 p_n}\right) \tag{A3}$$

Taking $N_{0,1}$ and $\bar{A}_1$ to be fixed reference values, it follows from Eq. (A3) that if $\log\{N(X)/a_n\}$ is plotted against X/p_n, a universal exceedance curve, independent of n, is obtained which depends only on the Gaussian-patch model parameters P_1, P_2, b_1, b_2 and the reference values $\bar{A}_1$ and $N_{0,1}$.

Referring to the implementation of the analysis method of Sec. II.B, it can be seen that if we identify the datum values $\bar{A}_1$ and $N_{0,1}$ with the linear filter designed to detect a single-ramp gust and $\bar{A}_n$ and $N_{0,n}$ with the filter designed to detect an n-ramp gust pattern, and take, in Eqs. (12) and (13), respectively,

$$a(n;q) = a_n \tag{A4}$$

and

$$p(n;q) = p_n \tag{A5}$$

not only will any pair of distributions $N(X)$, corresponding to different values of n, scale to share a common tangent for any arbitrary value of the moment-order parameter q, as in Fig. 4, but they will actually collapse to a single universal curve over the whole range of amplitudes, that is, the two curves in Fig. 4 will be coincident and represented by the single equation (A3). Thus, for the Gaussian-patch model, $a(n;q)$ and $p(n;q)$ take values a_n and p_n *independent of* q [Eqs. (A4) and (A5)].

Acknowledgments

Graham W. Foster of QinetiQ, Ltd., Bedford, was responsible for the management of the low-altitude turbulence data measurement program. Graham H. Watson of QinetiQ, Ltd., Farnborough, was responsible for the MATLAB implementation of the data-analysis algorithms. The high-altitude turbulence data (Sec. III.A) were kindly provided under a data-exchange agreement with NLR (National Aerospace Laboratory, the Netherlands, Peter van Gelder) and were used with the concurrence of NASA.

References

[1] Federal Aviation Regulations, "Part 25—Airworthiness Standards: Transport Category Airplanes," U.S. Department of Transportation, Federal Aviation Administration.

[2] Hoblit, F. M., *Gust Loads on Aircraft: Concepts and Applications*, AIAA Education Series, AIAA, New York, 1988.

[3] Houbolt, J. C., "Atmospheric Turbulence," (AIAA Dryden Research Lecture), *AIAA Journal*, Vol. 11, No. 4, 1973, pp. 421–437.

[4] Etkin, B., "Turbulent Wind and its Effect on Flight," *Journal of Aircraft*, Vol. 18, No. 5, 1981, pp. 327–345.

[5] Jones, J. G., "Documentation of the Linear Statistical Discrete Gust Method," U.S. Department of Transportation, Federal Aviation Administration, Office of Aviation Research Rept. DOT/FAA/AR-04/20, July 2004 [available for download from www.tc.faa.gov./its/worldpac/techrpt/ar04-20.pdf].

[6] Card, V., "Computer Simulation Studies of the Statistical Discrete Gust Method," Stirling Dynamics, Ltd., Rept. SDL-231-TR-4, May 1996 [available for download from www.stirling-dynamics.com/gust_documentation.htm].

[7] Jones, J. G., "Statistical Discrete Gust Method for Predicting Aircraft Loads and Dynamic Response," *Journal of Aircraft*, Vol. 26, No. 4, 1989, pp. 382–392.

[8] Chen, W.-Y., "Application of Rice's Exceedance Statistics to Atmospheric Turbulence," *AIAA Journal*, Vol. 10, No. 8, 1972, pp. 1103–1105.

[9] Frisch, U., *Turbulence, The Legacy of A.N. Kolmogorov*, Cambridge University Press, Cambridge, England, 1995.

[10] Jones, J. G., Foster, G. W., and Haynes, A., "Fractal Properties of Inertial Range Turbulence with Implications for Aircraft Response," *Aeronautical Journal of the Royal Aeronautical Society*, Vol. 92, Oct. 1988, pp. 301–308.

[11] Jones, J. G., Foster, G. W., and Earwicker, P. G., "Wavelet Analysis of Gust Structure in Measured Atmospheric Turbulence Data," *Journal of Aircraft*, Vol. 30, No. 1, 1993, pp. 94–99.

[12] Jones, J. G., Watson, G. H., and Foster, G. W., "Non-Gaussian Statistics of Atmospheric Turbulence and Related Effects on Aircraft Loads," *AIAA Journal*, Vol. 42, No. 12, 2004, pp. 2438–2447.

[13] Murrow, H. N., and Rhyne, R. H., "The MAT Project—Atmospheric Turbulence Measurements with Emphasis on Long Wavelengths," *Proceedings of the Sixth Conference on Aerospace and Aeronautical Meteorology of the American Meteorological Society*, American Meteorological Society, Boston, MA, Nov. 1974, pp. 313–316.

[14] Murrow, H. N., McCain, W. E., and Rhyne, R. H., "Power-Spectral Measurements of Clear-Air Turbulence to Long Wavelengths for Altitudes up to 14000 Metres," NASA TP-1979, April 1982.

[15] Foster, G. W., and Jones, J. G., "Analysis of Atmospheric Turbulence Measurements by Spectral and Discrete-Gust Methods," *Aeronautical Journal of the Royal Aeronautical Society*, Vol. 93, May 1989, pp. 162–176.

[16] Foster, G. W., and Jones, J. G., "Measurement and Analysis of Low Altitude Atmospheric Turbulence," AGARD Rept. R-734, Paper 2, 1987.

[17] Jones, J. G., "Studies of Time-Phased Vertical and Lateral Gusts : Development of Multiaxis One-Minus-Cosine Gust Model," U.S. Department of Transportation, Federal Aviation Administration, Office of Aviation Research Rept. DOT/FAA/AR-99/62, Oct. 1999 [available for download from www.tc.faa.gov./its/worldpac/techrpt/ar99-62.pdf].

[18] Wingrove, R. C., and Bach, R. E., "Severe Turbulence and Maneuvering From Airline Flight Records," *Journal of Aircraft*, Vol. 31, No. 4, 1994, pp. 753–760.

[19] Jones, J. G., "Measured Probability Parameters of Gust Patterns in Severe Turbulence," Stirling Dynamics, Inc. SDI-121-TR-3, July 2003 [available for download from www.stirling-dynamics.com/gust_documentation.htm].

[20] Jones, J. G., "A Unified Procedure for Meeting Power Spectral Density and Statistical Discrete Gust Requirements for Flight in Turbulence," AIAA Paper 86-1011, 1986.

[21] Perry, B., Pototzky, A. S., and Woods, J. A., "NASA Investigation of a Claimed 'Overlap' Between Two Gust Response Analysis Methods," *Journal of Aircraft*, Vol. 27, No. 7, 1990, pp. 605–611.

[22] Anandakumar, K., and Kailas, S. V., "Statistical Discrete Gust Analysis of Tower-Based Atmospheric Turbulence Data for Aircraft Response Studies," *Proceedings of the Institution of Mechanical Engineers, Part G (Journal of Aerospace Engineering)*, Vol. 213, 1999, pp. 143–162.